Rheological and Mechanical Relaxation Behavior of a Thermally Crosslinkable Poly(Ethylene Terephthalate)

PATRICK T. MATHER[1] *and* A. ROMO-URIBE[2,†]

[1]*Air Force Research Laboratory, Materials Directorate*
AFRL/MLBP
Wright Patterson AFB, Ohio 45433-7750

[2]*Systran Corp., Air Force Research Lab, Materials Directorate*
AFRL/MLBP
Wright Patterson AFB, Ohio 45433-7750

[†]*Now at: Hoechst Research and Technology*
US 86 Morris Ave.
Summit, New Jersey 07901

A novel terephthalic acid derivative based on benzocyclobutene, XTA, has been used as a comonomer in the preparation of thermally crosslinkable poly(ethylene terephthalate) copolymers. We have examined the rheological properties of a series of such polymers containing varying monomer percentages of the XTA comonomer: 0, 1, 5, 10, and 20. Incorporation of XTA into PET is found to cause dramatic changes in the temperature and time dependence of the rheological material functions, all indicating that the rate of crosslinking between chains in the melt increases as the XTA percentage is increased. The impact of thermal crosslinking on mechanical properties is also examined using dynamic mechanical analysis (DMA) on samples molded at a selected crosslinking temperature for times yielding varying levels of crosslinking extent. DMA results show that the activation energy of the β mechanical relaxation increases significantly, indicating the importance of torsional mobility of the aromatic ring of PET.

INTRODUCTION

Poly(ethylene terephthalate) PET, is a material of great commercial importance, in the form of fibers, bottle resin, and to a lesser extent, as a molding resin. In 1990, the annual world production of PET fibers was about 9 million metric tons and the annual world production of bottle resin was 1.2 million metric tons (1). Owing to the widespread use of PET, investigations of the decomposition routes and methods for reducing it flammability (Limiting Oxygen Index (LOI) $\approx$ 18%) have been a subject of significant effort over the past several decades (2). Past approaches for improving flame retardancy have included compounding with inorganic powders, such as antimony or phosphorous compounds, as well as halogen substitution along the polymer chains.

Recognizing the strong correlation between the tendency of a polymeric material to crosslink at elevated temperature and resulting "self-extinction," we have recently focused on the preparation of PET copolymers containing residues which upon exposure to extreme environments would lead to crosslinking and, in turn, decrease melt flow substantially. It is anticipated that such a reduction in melt flow would aid in the formation of a char and cessation of flame propagation (3). This effect has been demonstrated recently by incorporating a terephthalic acid derivative of benzocyclobutene (BCB), XTA, along the backbone of PET, the result being a favorable increase in LOI, from 18% to 33% (3). We note that materials with LOI $>$ 27% exhibit self-extinction under ambient atmospheric conditions.

The addition of latent crosslinking groups along the PET backbone is expected to affect not only flame retardancy, but rheological and mechanical properties as well. Previous research by the authors on thermotropic liquid crystalline polymers (LCPs) also containing XTA as a comonomer has shown that the time dependence of the rheological material functions at elevated temperature, as well as solid-state microstructure, are strongly affected by the mole fraction of XTA present in the system (4). In a similar fashion, many material characteristics are likely to be affected by XTA copolymerization in PET. One possibility is that

modification of the rheological properties of PET via branching below the gelation threshold may lead to enhanced "melt-strength" and/or a desirable time-dependence of melt-strength. Also, it is likely that the controlled introduction of chain branching either below or above the gelation threshold could improve the modulus and heat-deflection characteristics substantially, although only for mole percentages significantly larger than 50. The need for large mole percentages to enhance modulus has been demonstrated for PPTA-XTA copolymers in the past (5) and will be shown to be consistent with modulus data on PET-XTA copolymers in the present work.

Extensive examinations of the mechanical relaxation of PET have been conducted using dielectric (6–8) and dynamic mechanical (9, 10) analyses. These studies have revealed the presence of strong α and β relaxations, with the α relaxation occurring between 80°C and 105°C, depending on the degree of crystallinity, and the β transition, observed to be independent of the degree of crystallinity, being characterized by a broad loss peak centered near T = –55°C. By examining the frequency-dependence of the peak temperature for each mechanical transition (relaxation), estimations of the activation energy of the relaxations has been possible, yielding 184 kcal/mole for the α transition and a much lower 17 kcal/mole for the β transition. While the α transition is, as usual, taken to be related to concerted motion of large sections of the chain and cooperative motions between chains, the β transition appears to be less well understood, although indirect evidence points to the possibility that motions involving the ester moiety are important. Others have reported (11) that the loss peak observed in the vicinity of T = –55°C is a superposition of two peaks, one arising from ester motion and the other from the methylene units.

In this paper, we report the results of our investigation of the rheological and dynamic mechanical properties of PET copolymers containing varying monomer percentages of the XTA comonomer: 0, 1, 5, 10, and 20 mole percent. Rheological experiments are intended to define the processability of the material, as well as to examine the kinetics and nature of the crosslinking reaction taking place. Dynamic mechanical measurements are performed to quantify the modification of the mechanical properties and molecular relaxation characteristics resulting from the addition of the XTA comonomer.

EXPERIMENTAL

Synthesis of PET and PET-co-XTA Copolymers

The neat PET polymer and PET-co-XTA copolymers were synthesized using a two step process. The chemical structure of the polymers is shown below, where the sequence distribution is believed to be relatively random due to the similar reactivity of XTA and terephthalic acid.

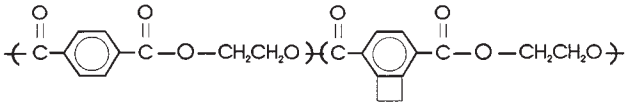

A two-necked reaction vessel was specially adapted for this procedure. It contained a 24/40 and a 29/42 joint. Into the 29/42 joint a four-necked (19/20) adapter was added. The stirring shaft entered through one of the smaller joints. A short path distillation condenser was attached to the 24/40 joint. Heating was done using a Corning stirrer/heater and a Wood's metal bath. All reactants were used as-received from Aldrich. The XTA diester monomer was synthesized previously (12,13). A Caframo high speed, high torque motor with a stainless steel stirring shaft was used to stir the system.

First, ethylene glycol (1.29 moles, 80.07 gm), dimethyl terephthalate (0.522 mole, 101.37 gm), and zinc acetate (2.6×10^{-4} mole, 0.057 gm) were combined and heated to 180°C. As the reaction proceeded, methanol was released and an aspirator vacuum was used to facilitate its removal. This first step generally took about 3 hours to complete and resulted in a clear reaction mixture. After a stoichiometric amount of methanol was removed from the system, the second step began. Antimony trioxide (2.3×10^{-4} mole, 0.067 gm) and triphenyl phosphate (2.2×10^{-4} mole, 0.072 gm) were added to the system, along with several mL of ethylene glycol to wash them into the reaction vessel. The temperature was increased to 280°C. Ethylene glycol started to distill over anywhere between 240°C up to 280°C. An aspirator vacuum was used to remove as much of the ethylene glycol as possible, then a higher vacuum (approx. 200 mm Hg) was used to remove the rest of it. This second step took 4–6 hours to complete (14, 15). If the molecular weight was not high enough, a third step was employed. This involved taking the already made polymer and heating it to the molten state under a higher vacuum (~60 mm Hg) using a dry ice condenser to collect the ethylene glycol. Once the polymer reached a higher molecular weight, it was much more viscous and slightly yellow in color.

The procedure to make PET-co-XTA was the same as above with only a few variations. The XTA monomer was added in the various mole percentages in the first step. Careful control of the reaction temperature below 280°C was critical to avoid the BCB crosslinking reaction. If temperatures were higher than that for any significant amount of time, the polymer would crosslink into a tough, insoluble mass in the reaction vessel. This became more of a problem for the higher mole percentages of XTA. The PET-co-XTA polymers were a green color, which increased in intensity as the XTA content increased. This may have been due to increased conjugation from small amounts of crosslinking during synthesis.

The copolymers are named PET-co-*n*XTA, where *n* refers to the mole percentage of XTA comonomer used in the synthesis. We refer to the PET homopolymer synthesized for this study at PET-co-0XTA to distinguish it from the commercial PET sample. For simplicity, the copolymer containing 4.8 mole percent XTA is referred to as PET-co-5XTA.

Intrinsic Viscosity Measurements

Intrinsic viscosity measurements were made using a Cannon 50 E264 viscometer at 25°C in *o*-chlorophenol. The intrinsic viscosity was determined by plotting specific viscosity, normalized by concentration, versus concentration and extrapolating to zero. Molecular weight was determined by using the Mark-Houwink equation, $[\eta] = kM^a$ (k and $a = 6.56 \times 10^{-4}$ and 0.73, respectively)(16). It was assumed that the molecular weight relationship for the PET-co-XTA copolymers was the same as for the neat PET.

Morphological Characterization

The morphological characterization of the PET-co-XTA copolymers was performed by using wide-angle X-ray scattering (WAXS) with a flat-plate Statton camera. The samples were prepared by compression molding the samples at a temperature less than the polymer melting point, but significantly higher than the glass transition, typically $T = 225$°C. A pressure of 15 MPa was applied to the heated compression mold for 2 minutes and the mold was then cooled under pressure to room temperature at a rate of approximately 2°C/min. A Rigaku rotating anode X-ray generator was employed with a *Cu* target and graphite monochromator. The film processing was standardized and the *d*-spacings were calibrated with silicon powder. X-ray films were digitized using a Molecular Dynamics microdensitometer to convert photographic blackening to optical density, and the densities then corrected for polarization, absorption, and geometrical factors.

Rheological Characterization

Rheological characterization was performed using a Rheometrics RMS-605 rheometer fitted with opposing 25 mm parallel disks and operated in dynamic mode. Samples for rheological analysis were prepared by vacuum compression molding disks at 260°C for periods not exceeding 4 minutes using a mold piston pressure of 15 MPa. The mold was quickly cooled and the sample removed for storage in a vacuum oven until testing. Both heating and isothermal rheological experiments were performed. In the isothermal experiments, care was taken to begin data acquisition of the material functions as quickly as possible and, as such, early time data reflect the changing (temperature) in the environmental chamber. For data presented under these circumstances, the temperature is also reported.

Dynamic Mechanical Analysis

Dynamic mechanical analysis was performed using the RMS-605 rheometer in the torsion-cylinder geometry using custom grips made in our laboratory which utilize pin-vises (McMaster Carr) adapted to standard Rheometrics fixtures. Samples for DMA testing were compression molded using a cylindrical mold with a two-piece strand insert, yielding samples approximately 3 cm in length and 2mm in diameter. Temperatures and annealing times were selected based on crosslinking kinetics measured in the melt rheology experiments.

RESULTS AND DISCUSSION

Molecular Weight Characterization

A summary of the viscosity and molecular weight data is displayed in *Table 1*. Also shown in *Table 1* is the number of XTA groups per chain, N_x, calculated from the mole percentage used in the synthesis and the measured viscosity-average molecular weight. As the XTA content was increased, the molecular weight of the polymers decreased. This can be attributed to the competing processes of crosslinking versus chain extension during the final stages of the synthesis, forcing systematic decrease of the polymerization time at 280°C. In comparison to a commercial sample, molecular weights of the polymers under study are quite low: a sample of PET (from Hoechst Celanese) was found to have an intrinsic viscosity of 0.93 yielding a viscosity-average molecular weight of 20,600. Despite the low molecular weights, all of the polymer

Table 1. Summary of Intrinsic Viscosity,[a] Molecular Weight,[b] and XTA/Chain[c] Data for PET-co-XTA Polymers.

Compound	Viscosity (dL/g)	Molecular Weight (g/mol)	N_x = XTA Groups/Chain
PET (neat)	0.52	9400	0.0
PET-co-1XTA	0.48	8400	0.4
PET-co-5XTA	0.47	8200	2.2
PET-co-10XTA	0.25	3400	1.8
PET-co-20XTA	0.23	3100	3.2

[a] Measured in o-chlorophenol at 25°C.
[b] Viscosity-average molecular weight estimated from the Mark-Houwink formula for PET.
[c] Estimated from XTA mole-fractions used in the synthesis and degrees-of-polymerization computed from viscosity-average molecular weight data. Values are expected to be accurate to ±0.25.

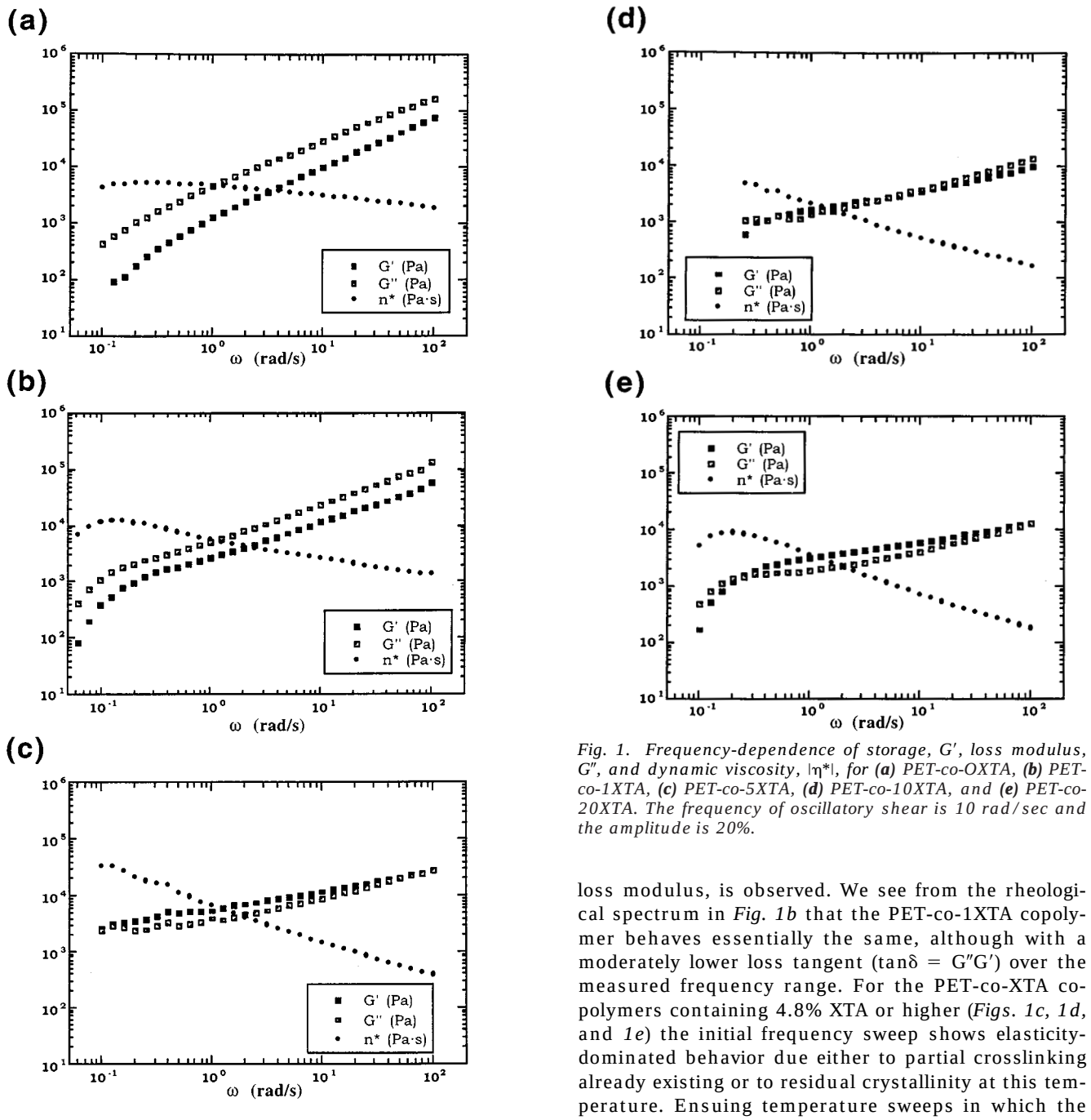

Fig. 1. Frequency-dependence of storage, G′, loss modulus, G″, and dynamic viscosity, |η|, for* ***(a)*** *PET-co-OXTA,* ***(b)*** *PET-co-1XTA,* ***(c)*** *PET-co-5XTA,* ***(d)*** *PET-co-10XTA, and* ***(e)*** *PET-co-20XTA. The frequency of oscillatory shear is 10 rad/sec and the amplitude is 20%.*

samples were readily melt-spun into fibers for the purposes of another study.

Rheological Characterization

Shown in *Fig. 1* are frequency sweeps of each PET copolymer at 257°C, just after loading the samples in the rheometer. The PET-co-0XTA copolymer is observed to behave as a viscous liquid, as seen in *Fig. 1a*, for frequencies less than ~0.5 rad/sec, with a mechanical spectrum indicative of a broad molecular weight distribution and a molecular weight below the critical molecular weight for entanglement coupling; i.e., no rubbery plateau, nor a crossing of storage and loss modulus, is observed. We see from the rheological spectrum in *Fig. 1b* that the PET-co-1XTA copolymer behaves essentially the same, although with a moderately lower loss tangent ($\tan\delta = G''G'$) over the measured frequency range. For the PET-co-XTA copolymers containing 4.8% XTA or higher (*Figs. 1c, 1d,* and *1e*) the initial frequency sweep shows elasticity-dominated behavior due either to partial crosslinking already existing or to residual crystallinity at this temperature. Ensuing temperature sweeps in which the rheological material functions are monitored with increasing temperature at 10 rad/sec lend insight on this behavior, as described below.

Figure 2 summarizes the temperature dependence of the rheological material functions of the PET-XTA copolymers as measured at 10 rad/sec from 257°C to 350°C using a heating rate of 5°C/min. It should be noted that the choice of 5°C/min was somewhat arbitrary and other choices should lead to qualitatively similar curves with some quantitative differences based on the kinetic nature of the experiment. In *Fig. 2a* and *2b* we see that three regimes of temperature behavior are observed for both the PET-co-0XTA and PET-co-1XTA copolymers. Regime I, spanning a tem-

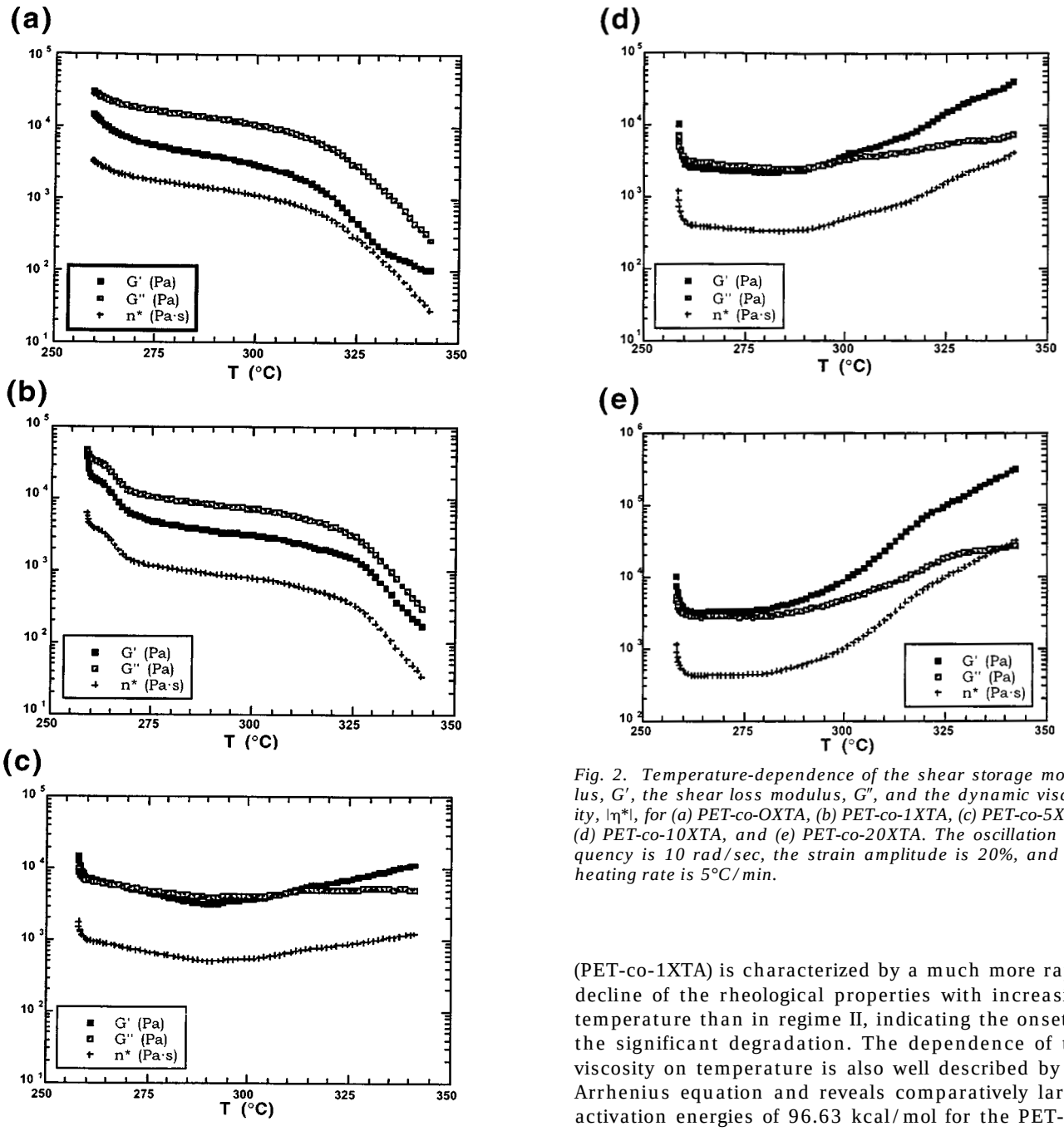

Fig. 2. Temperature-dependence of the shear storage modulus, G′, the shear loss modulus, G″, and the dynamic viscosity, |η|, for (a) PET-co-OXTA, (b) PET-co-1XTA, (c) PET-co-5XTA, (d) PET-co-10XTA, and (e) PET-co-20XTA. The oscillation frequency is 10 rad/sec, the strain amplitude is 20%, and the heating rate is 5°C/min.*

perature range of 257°C to roughly 270°C, consists of rapidly declining storage and loss modulus, most likely due to the completion of sample melting. Regime II, extending from 270°C to 310°C (PET-co-0XTA) or 320°C (PET-co-1XTA) features a monotonic reduction of the magnitude of the rheological material functions typical of most liquids. The viscosity data within this regime are adequately described by an Arrhenius model with extracted activation energies of 10.28 kcal/mol for PET-co-0XTA and 10.11 kcal/mole for PET-co-1XTA, Regime III, covering temperatures greater than 310°C (PET-co-0XTA) or greater than 320°C (PET-co-1XTA) is characterized by a much more rapid decline of the rheological properties with increasing temperature than in regime II, indicating the onset of the significant degradation. The dependence of the viscosity on temperature is also well described by an Arrhenius equation and reveals comparatively larger activation energies of 96.63 kcal/mol for the PET-co-0XTA copolymer and 108.82 kcal/mol for the PET-co-1XTA copolymer. For both PET-co-0XTA and PET-co-1XTA, the shear loss modulus remains substantially less than the storage modulus for the full range of temperature explored.

Copolymers containing higher levels of XTA showed qualitatively different behavior in the temperature-sweep experiments. In particular, the PET-co-5XTA copolymer displays a clear minimum in dynamic viscosity versus temperature curve and, for temperatures higher than this minimum, the viscosity increases with a slope comparable in magnitude with the downward slope at lower temperatures. Unlike the copolymers containing lower amounts of XTA comon-

omer, the respective evolution of the shear storage and loss modulus show two crossings with increasing temperature. While the storage modulus starts out to be slightly larger than the loss modulus at T = 255°C, it has a stronger temperature dependence (larger negative slope) such that the two cross near T = 265°C. With further increase in the temperature, all three rheological material functions reach a minimum at 292°C and the storage modulus begins to rise with temperature with a larger slope than does the loss modulus. The storage modulus crosses the loss modulus at 308°C and, above 315°C, the loss modulus reaches an asymptotic value of 5500 Pa while the storage modulus continues to rise with temperature reaching 12,000 Pa at 350°C.

The PET-co-10XTA copolymer shows a temperature dependence of the rheological properties similar to that of the PET-co-5XTA sample, except for several key features. First, lower negative slopes are observed for material functions at low temperatures and the loss modulus is greater than the storage modulus for temperatures just above the melting point. The storage modulus begins to rise with increasing temperature above T = 285°C. The crossing of the storage modulus over the loss modulus with increasing temperature occurs at a lower temperature of 293°C (compared with 308°C for PET-co-5XTA) and the storage modulus increases with temperature at a significantly higher rate than the PET-co-5XTA sample.

PET-co-20XTA shows a temperature profile indicating that the storage modulus is always larger than the loss modulus, such that no crossover of storage and loss modulus occurs, although comparison with the other samples can be made on the basis of the temperature above which the storage modulus is observed to increase with temperature, which is 275°C for 20XTA compared with 285°C observed for the 10XTA sample. In addition, the rate of increase in storage modulus with temperature is highest for 20XTA relative to the other polymers.

Shown in *Fig. 3* are the viscosity versus temperature curves for all five copolymers showing two significant trends with increasing XTA comonomer fraction. First, the viscosity at low temperatures is observed to decrease systematically with increasing XTA mole fraction. This is consistent with our measurements of a lower intrinsic viscosity, and thus average molecular weight, for copolymers with increasing XTA content. We recall that in order to prevent crosslinking during the melt polymerization reactions, larger XTA contents mandated short reaction times, thus resulting in systematically lower molecular weights. The second trend indicated by the viscosity curves in *Fig. 3* is the substantial increase in the positive slope of viscosity versus temperature with increasing XTA mole fraction. Deviation from a downward trend in viscosity with increasing temperature is very likely due to crosslinking of chains by the BCB-BCB coupling reaction which, depending on the relative location of the XTA comonomers along the chains, may act as steps of branching, chain extension, cyclization, gelation, and finally network refinement.

The rheological material functions were monitored versus time for several of the PET copolymers, as well as for a commercial-grade PET resin (17). The evolution of the rheological material functions with time were quite similar for PET-co-0XTA (*Fig. 4)* and PET-co-1XTA (*Fig. 5*) for T = 275°C and ω = 10 rad/sec. In fact, based on data reported previously on commercial PET resin at 280°C (18), it was anticipated that thermal treatment would lead to viscosity reduction with time, rather than the observed increase in viscosity

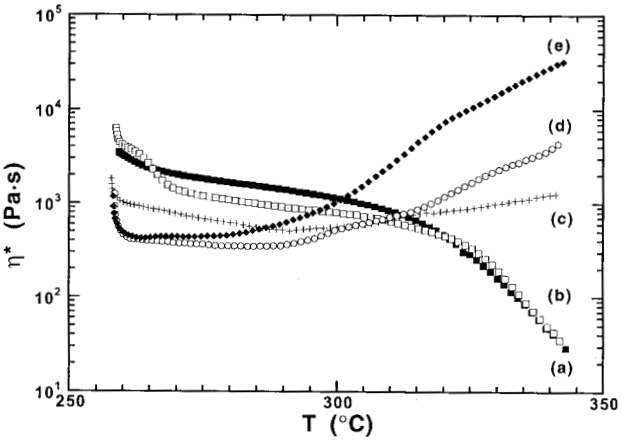

Fig. 3. Temperature-dependence of the dynamic viscosity, |η|, for (a) PET-co-OXTA, (b) PET-co-1XTA, (c) PET-co-5XTA, (d) PET-co-10XTA, and (e) PET-co-20XTA. The oscillation frequency is 10 rad/sec, the strain amplitude is 20%, and the heating rate is 5°C/min.*

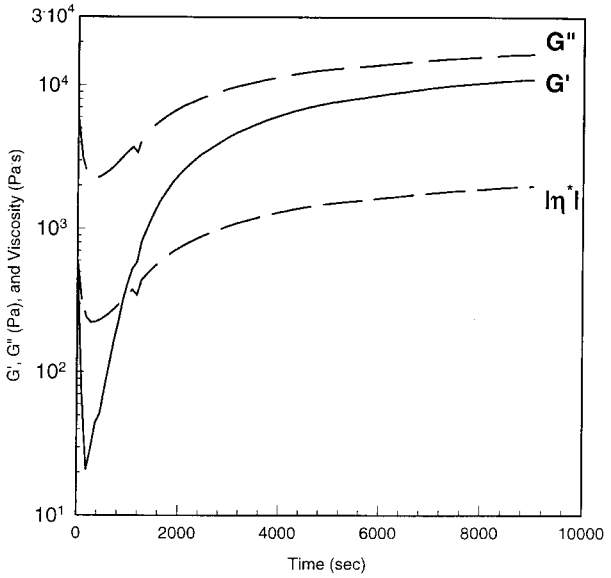

Fig. 4. Time dependence of rheological material functions of PET-co-OXTA at T = 275°C. The oscillation frequency is 10 rad/sec and the strain amplitude, determined to be within linear limits, is 10%.

with time. It seems likely, however, that viscosity reduction with time should increase with shear stress, which is quite small in this case. The commercial PET resins examined by Kiang and Cuculo ranged in average molecular weight from 25,000 g/mol to 70,000 g/mol, the lower molecular weight showing the least reduction in viscosity with time. The molecular weight for the PET polymer examined in this study was significantly lower at approximately 10,000 g/mol, yielding an average degree of polymerization (DP) as low as 50.

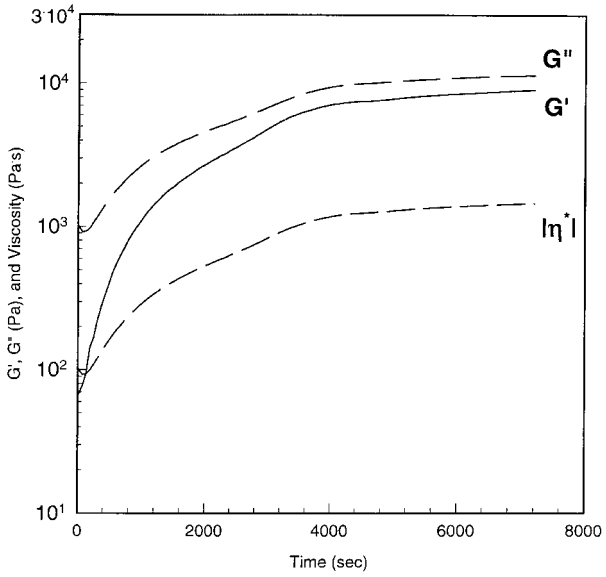

Fig. 5. Time dependence of the rheological material functions of PET-co-1XTA at T = 275°C. The oscillation frequency is 10 rad/sec and the strain amplitude, determined to be within linear limits, is 20%.

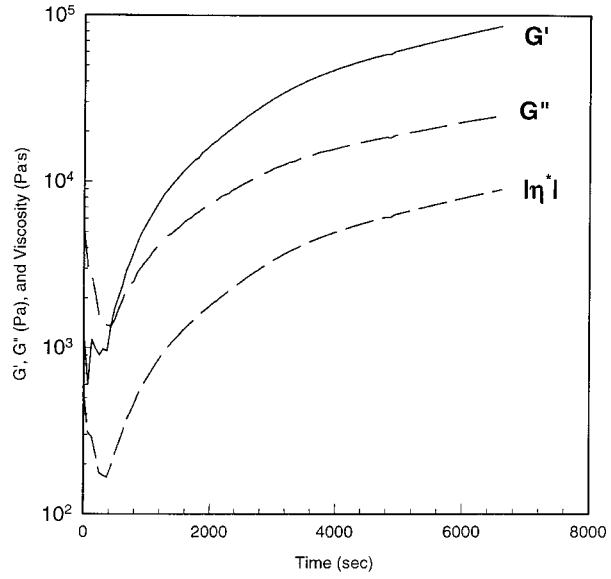

Fig. 6. Time dependence of the rheological material functions of PET-co-5XTA at T = 275°C. The oscillation frequency is 10 rad/sec and the strain amplitude is 2%.

Figures 4 and *5* also show that while annealing at 275°C for up to 150 minutes G′ gradually converges with G″ for ω = 10 rad/sec, but the two never cross and the asymptotic value of the shear loss tangent is approximately 1.8 for PET-co-0XTA and 1.2 for PET-co-1XTA. It is expected for a material crossing a gelation threshold that the storage modulus should cross the loss modulus for all frequencies (19), and this is clearly not possible for both samples shown in *Figs. 4* and *5*, respectively.

Figure 6 shows the evolution of the rheological properties of PET-co-5XTA at 275°C, where significant qualitative differences appear in comparison to copolymers PET-co-0XTA and PET-co-1XTA. The first major difference is that at a very early stage of annealing, approximately 8 minutes, the storage modulus crosses the loss modulus, an observation consistent with transformation to solid-like behavior as measured at 10 rad/sec. Secondly, the increase in viscosity (as well as G′ and G″) with time is sustained for a longer duration than in PET-co-0XTA and PET-co-1XTA. Finally, the rate of change in the rheological properties with time is observed to be significantly higher in the PET-co-5XTA copolymer, apparently a result of the substantially higher concentration of reactive sites, as well as the relatively higher reactivity of the BCB group as compared to transesterification at 275°C, although this hypothesis was not tested.

The viscosity data from *Figs. 4*, *5*, and *6* are summarized in *Fig. 7*, along with the evolution of the dynamic viscosity of the commercial PET resin. The commercial resin, while displaying a larger viscosity at early times and throughout the annealing (due to a

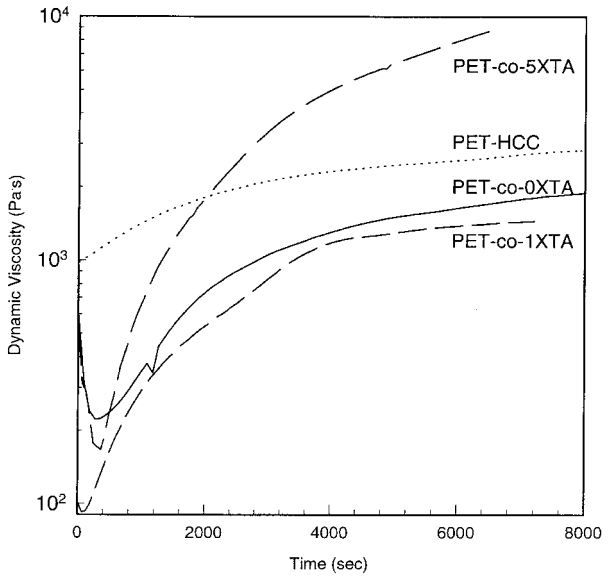

Fig. 7. Comparison of the dynamic viscosity evolution at 275°C for all of the PET-co-XTA copolymers, as well as a commercial grade PET. The oscillation frequency is 10 rad/sec and the strain amplitude varies from 2% (5XTA) to 20% (1XTA).

higher molecular weight) shows a similar time dependence. It is noted additionally that the shear loss tangent for the polymer approaches an asymptotic value of approximately 3. Clearly, a transition exists in the annealing behavior between XTA mole fractions of 1% and 5%, this likely arising from a simple percolation concept which we now describe. From the intrinsic viscosity data, we estimate the average degree of polymerization (DP) of the XTA copolymers to range from 44 (PET-co-0XTA) to 16 (PET-co-20XTA). Considering the mole percentage of repeat units containing the XTA group, as well as the measured molecular weight, we have estimated the number of XTA groups per chain, N_x, as shown in *Table 1*. Because N_x must exceed 2 for gelation upon complete reaction, the PET-co-0XTA and PET-co-1XTA samples are not expected to reach gelation, while the other samples should, in agreement with our observations. We note that for PET-co-10XTA, $N_x = 1.8 \pm 0.25$, is within the gelation threshold considering the level of error in the estimation of N_x.

Dynamic Mechanical Analysis

The PET-co-5XTA samples were annealed in the melt at 275°C for either 2 minutes or for 2 hours and the effects of this heat treatment on mechanical relaxation were examined. *Figure 8* shows the mechanical relaxation spectra for PET-co-5XTA melt processed so that minimal time at the processing temperature (275°C) was achieved. The plots feature the dependence of the shear storage and loss moduli on temperature for frequencies of (a) 100, (b) 10, and (c) 1 rad/sec. The mechanical relaxation spectra show a weak decrease in storage modulus with temperature for the range of –100°C up to about 75°C, where an abrupt decrease in storage modulus is observed. This temperature is regarded as an α-relaxation, based on its close proximity to the α-relaxation observed in PET as well as on the magnitude of the G'' peak (and small frequency dependence). Above the α transition, the shear storage modulus decreases with a large temperature dependence up to about 130°C, at which point the negative slope decreases significantly. The loss modulus vs. temperature traces show dramatically the presence of both α and β mechanical relaxations. In both cases, the temperature corresponding to the peak in G'' was found to be dependent on the oscillation frequency, as expected, although the frequency dependence of the β-transition temperature was larger than that observed in previous studies of PET. Possible explanations include the effect of low molecular weight, such as a large concentration of end groups. No significant alteration of the PET mechanical spectrum was observed, indicating that unreacted BCB groups do not relax within the temperature-frequency range explored.

It is also observed for all three oscillation frequencies that the temperature corresponding to the α transition is lower for the 120 minute anneal, but that the shear storage modulus above the α transition temperature is consistently higher for the 120 minute anneal as compared to the 2 minute anneal. The latter observation agrees with the data shown in *Fig. 7* in which, at 275° C, the shear storage modulus is observed to

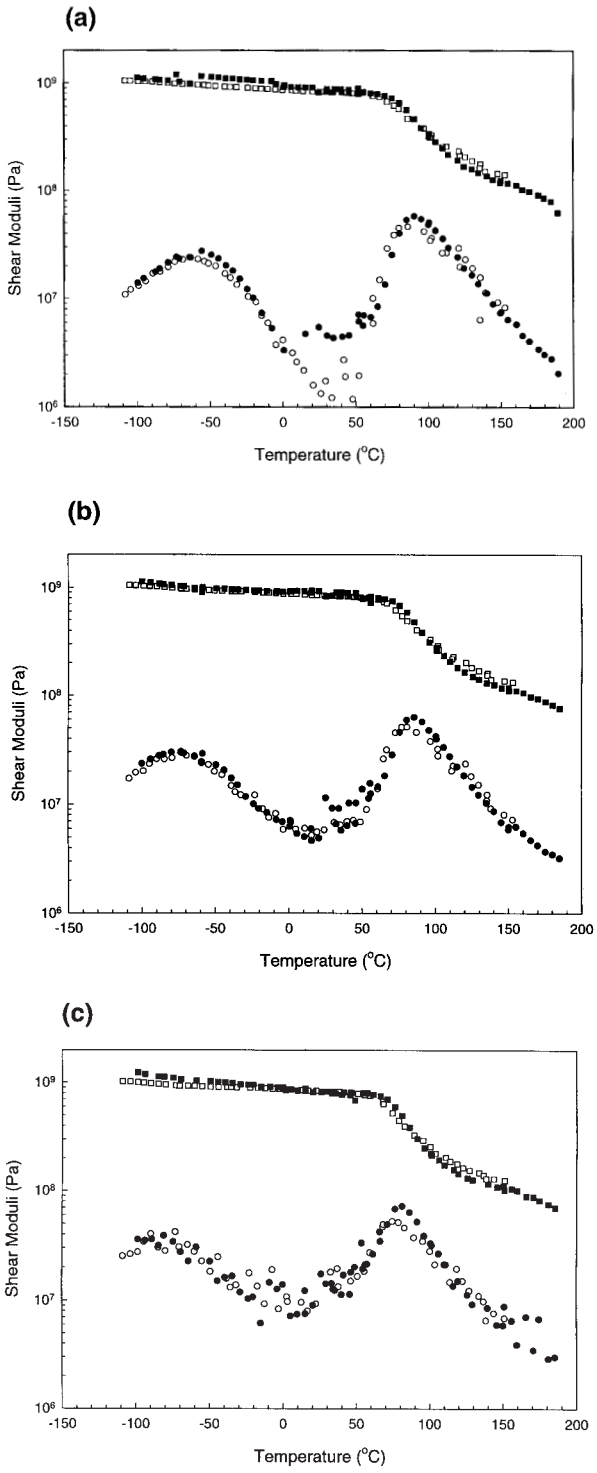

Fig. 8. Temperature dependence of the shear storage (□) and shear loss (○) moduli of PET-co-5XTA molded at 275°C for 2 minutes (filled symbols) and for 120 minutes (open symbols). The oscillation frequency is (a) 100 (b) 10, and (c) 1 rad/sec.

increase by a factor of about 50 if annealed for 120 minutes. Thus, if the DMA data shown in *Fig. 8* were extended to 275°C (which is exceedingly difficult with a single sample geometry) it is expected that the G'-temperature traces for the 2 minute and 120 minute anneals would diverge to ultimately agree with the data presented in *Fig. 7,* assuming a fast heating rate to 275°C. In other words, the modulus of the 5XTA sample, with most of the XTA groups reacted (120 minute anneal), most dramatically exceeds that of the uncrosslinked sample at temperatures higher than the α relaxation temperature, while at lower temperatures no significant difference in the storage moduli is observed.

From the data shown in *Fig. 8,* the activation energy for both the α and β transitions were estimated for samples annealed for 2 minutes and 120 minutes at 275°C, respectively, using the peaks in G''-temperature plots and the results are shown in *Fig. 9*. The oscillation time constant ($\tau = 2\pi/\omega$) is plotted versus the inverse of the temperature corresponding to a peak in the G''-temperature curve for the α transition (closed symbol) and the β transition (open symbol). Plotting the data as shown allows the determination of transition activation energies of 124.3 kcal/mol for the α relaxation and either 8.52 kcal/mol (2 minute anneal) or 18.42 kcal/mol (120 minute anneal) for the β relaxation. While these values seem reasonable when compared to previous results for poly(ethylene terephthalate) (10, see Introduction), it should be emphasized that the values were extracted from frequency spectra spanning only two decades of time scale and that more accurate values would be obtained from a broader time-scale range that is experimentally more accessible with dielectric spectroscopy. The increase in the activation energy of the β transition with annealing is surprising, and likely arises from an impact of interchain crosslinking on the freedom of motion of neighboring bonds, such at the ester or methylene groups.

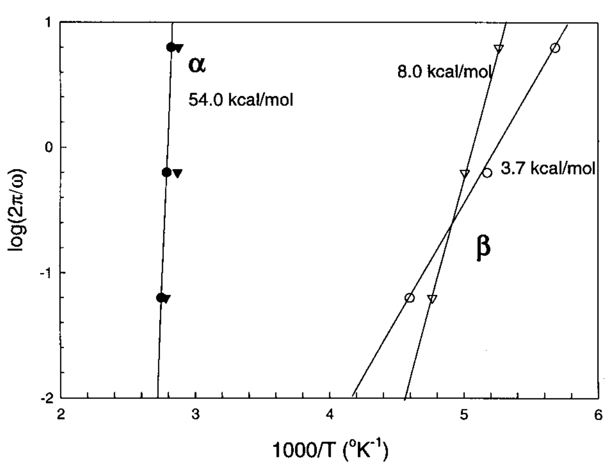

Fig. 9. Arrhenius plots yielding the activation energies of the α (filled) and β (open) mechanical relaxations for the 5XTA sample annealed for 2 minutes (○) and for 120 minutes (∇) at 275°C.

In *Fig. 10*, we depict the two neighboring PET chains which have been crosslinked via ring opening of the BCB groups (3). Rotation about ϕ_1 and neighboring bonds between aromatic rings may be affected by phenyl ring coupling due to crosslinking. In particular, the moderate increase in activation energy of the β relaxation on crosslinking suggests that torsional mobility of the terephthalate residue plays an important role in the transition and does not involve simply the activation of torsional rotations within the ester and methylene groups. This is in contrast to the conclusions of Tatsumi, Ito, and Hayakawa based on dielectric analysis of PET (8).

Morphological Characterization

Figure 11 shows wide-angle X-ray scattering patterns of as-molded PET and uncrosslinked PET-co-XTA copolymers. The PET pattern confirms the semicrystalline nature of the material; it also looks slightly anisotropic, a reflection of the mechanical history associated with the sample preparation method. On the other hand, the Debye-Scherrer rings in PET-co-XTA copolymers confirm that the materials are polycrystalline, orientationally isotropic, and possess a crystalline structure resembling that of PET, which is triclinic (20). There are subtle features in these patterns that can be better appreciated from their intensity traces, *Fig. 12a*. First, we note that the degree of crystallinity in the copolymers is significant in all cases (intense reflections, narrow in 2θ), and increases as XTA content increases, up to about 10%. However, at 20% XTA content the crystallinity is noticeably diminished. The degree of crystallinity has been quantified according to the method described by Ruland (21) and the results are shown in *Fig. 12b* where the degree of crystallinity is plotted as a function of XTA content. From *Fig. 12a* we also note that the diffraction peaks are shifting gradually to smaller angles with increase of XTA content. The reduction in crystallinity is most likely associated to the random nature of the copolymers and the fact that the crosslinkable groups disrupt macromolecular packing. This effect is more marked at higher XTA concentrations, where at 50% XTA content the polymer is completely amorphous (3).

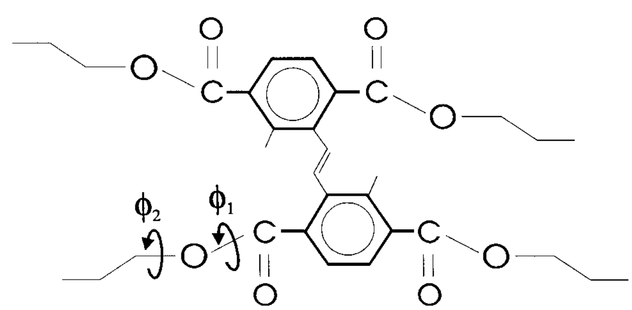

Fig. 10. Schematic of two neighboring PET chains that have been coupled via a BCB-BCB crosslinking reaction. ϕ_1 and ϕ_2 are torsional angles about which rotation may be activated during the β relaxation process.

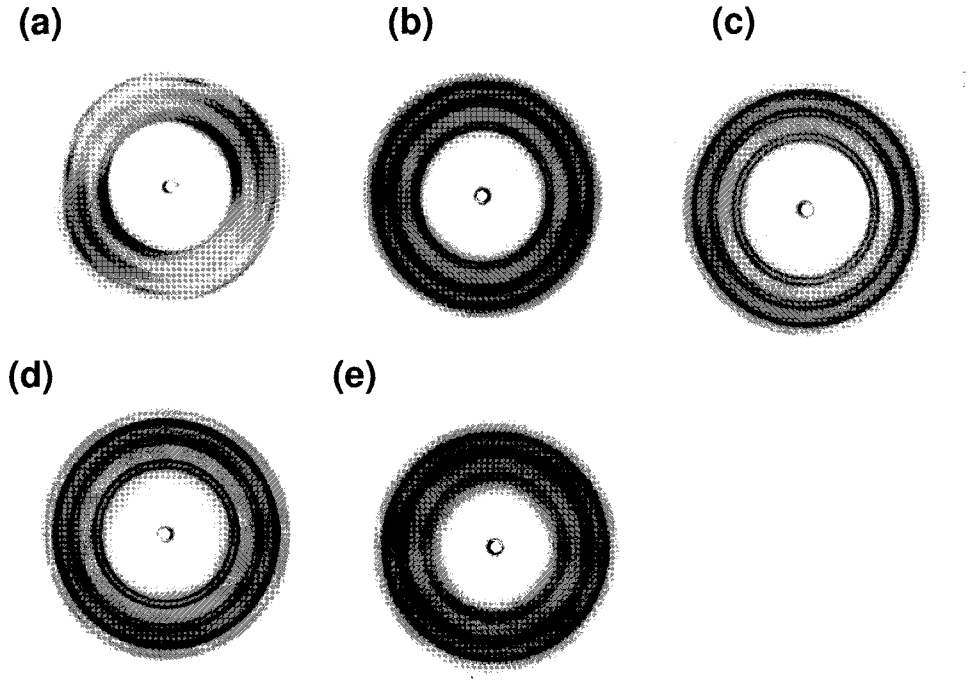

Fig. 11. Wide-angle X-ray scattering (WAXS) patterns of: (a) PET-co-OXTA, (b) PET-co-1XTA, (c) PET-co-5XTA, (d) PET-co-10XTA, and (e) PET-co-20XTA.

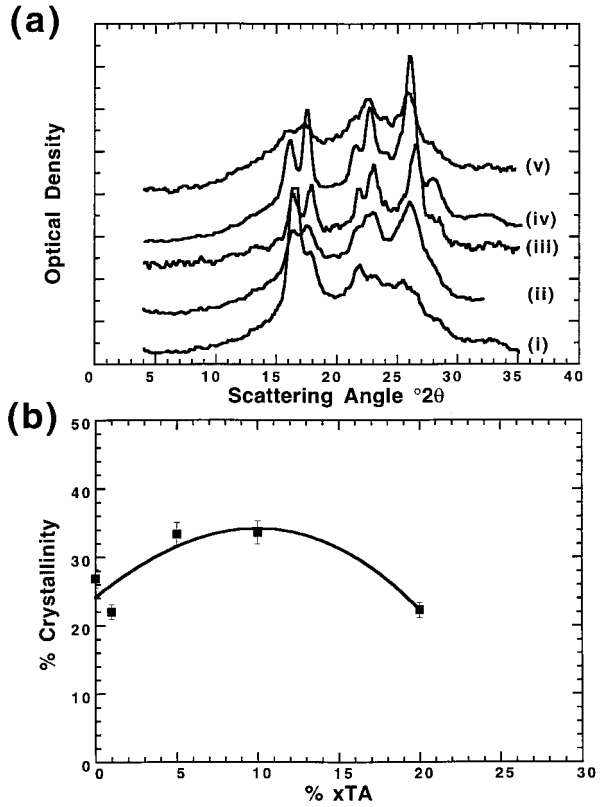

*Fig. 12. **(a)** Line profiles of wide-angle X-ray scattering (WAXS) data shown in Fig. 11: (i) PET-co-OXTA, (ii) PET-co-1XTA, (iii) PET-co-5XTA, (iv) PET-co-10XTA, and (v) PET-co-20XTA. (b) Percentage crystallinity versus mole-percentage XTA co-monomer.*

On the other hand, the fact that the structure in the copolymers resembles that of plain PET is not surprising. Lu and Windle (22) have shown that, in copolymers of PET and poly(ethylene naphthalene-2,6-dicarboxylate)—PEN—the unit cell of the crystalline structure corresponds to that of PET, up to 20 mol% content of PEN. They have also reported that the unit cell will change to that of PEN at higher PEN concentrations.

We have also examined the effect of crosslinking on the microstructure of the PET-co-5XTA copolymer and the results are shown in *Fig. 13*. The solid line corre-

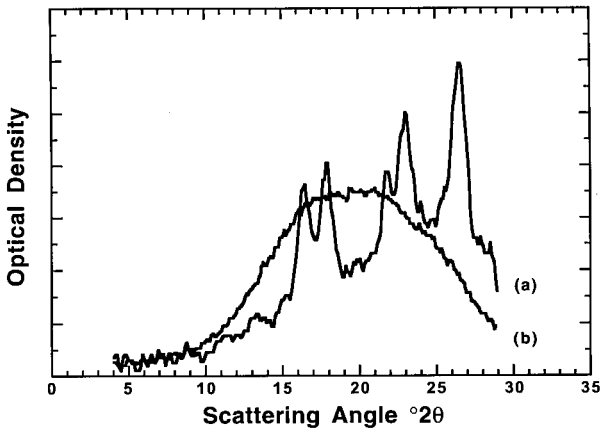

Fig. 13. Line profiles of wide-angle X-ray scattering (WAXS) patterns for PET-co-5XTA at room temperature (a) before crosslinking, and (b) after crosslinking at 275°C for 120 minutes.

sponds to the sample being pressed at a temperature below its melting point. The dashed line, however, corresponds to a sample that was annealed at 275°C for 120 minutes, the same conditions used for the DMA results shown in *Fig. 9*. The broad amorphous halo shows that the crosslinking reaction occurring in the molten copolymer has suppressed its ability to crystallize.

CONCLUSIONS

1. We have found that the inclusion of XTA comonomer in poly(ethylene terephthalate) leads to interchain crosslinking, as evidenced by rheological characterization, with the rate of crosslinking increasing with XTA mole fraction.
2. The evolution of viscosity with time during crosslinking showed a strong transition from 1 wt% XTA to 5 wt% XTA. Along with molecular weight assessments from intrinsic viscosity data, this results from the surpassing of two XTA groups per chain as required for percolation gelation to occur.
3. Crosslinking of the PET-co-5XTA copolymer had very little effect on the magnitude of the shear storage modulus in the solid state, as measured using dynamic mechanical analysis, although the magnitude of the activation energy for the β transition ($T \sim -75$°C) increased on crosslinking from 8.5 kcal/mol to 18.4 kcal per mole. This increase in activation energy is consistent with the concept that torsional mobility of the aromatic ring in PET is important in the β relaxation.
4. Copolymerization of XTA in PET leads to some alteration of the microstructure, particularly by altering the degree of crystallinity resulting from a particular thermal history and slightly shifting the diffraction peaks to lower angles. Crosslinking of the PET-co-5XTA sample, however, led to complete suppression of crystallization.

ACKNOWLEDGMENTS

Hoechst Celanese Corporation kindly supplied the commercial PET resin. This research was supported by the Air Force Office of Scientific Research.

REFERENCES

1. A. J. East, chapter entitled: "Polyesters, Thermoplastic" from Kirk-Othmer *Encyclopedia of Chemical Technology*, Fourth Edition.
2. P. H. Chang and C. A. Wilkie, *J. Appl. Polym. Sci.,* 38, 2245 (1989).
3 B. J. Foran, E. Pingel, G. E. Spilman, L. J. Markoski, T. Jiang, and D. C. Martin, *Mater. Res. Soc. Proc.,* 461, 223 (1997).
4 P. T. Mather, K. P. Chaffee, A. Romo-Uribe, G. Spilman, T. Jiang, and D. C. Martin, *Polymer,* 38, 6009 (1997).
5 M.-C. Jones, T. Jiang, and D. C. Martin, *Macromolecules,* 27, 6507 (1995).
6 W. Reddish, *Trans. Faraday Soc.,* 46, 459 (1950).
7 S. Saito, *Kolloid Z.,* 189, 116 (1963).
8 T. Tatsumi, E. Ito, and R. Hayakawa, *J. Polym. Sci.: Part B: Polym. Phys.,* 30, 701 (1992).
9 K. H. Illers and H. Breuer, *Kolloid Z.,* 176, 110 (1961).
10 K. H. Illers and H. Breuer, *J. Colloid. Sci.,* 18, 1 (1963).
11 I. Okazaki and B. Wunderlich, *J. Polym. Sci. B. Polym. Phys.,* 34, 2941 (1996).
12 K. A. Walker, L. J. Markoski, and J. S. Moore, *Synthesis*, 12, 1265 (1992).
13 K. A. Walker, L. J. Markoski, and J. S. Moore, *Macromolecules,* 26, 3713 (1993).
14 H. F. Mark, N. M. Bikales, C. G. Overberger, G. Menges, and J. I. Kroschwitz, *Encyclopedia of Polymer Science and Engineering,* 2nd Ed., 12, John Wiley and Sons (1988).
15 H. R. Billica, U.S. Patent 2,647,885 (1951).
16 E. L. Lawton and E. L. Ringwald, *Polymer Handbook,* 3rd Edition, V101–105, J. Brandrup and E. H. Immergut, eds., Wiley, New York (1989).
17 PET lot 39110, Hoechst Celanese Corporation.
18 C. T. Kiang and J. A. Cuculo, *J. Appl. Polym. Sci.,* 46, 55 (1992).
19 M. DeRosa and H. H. Winter, *Rheol. Acta,* 33, 220 (1994).
20 R. P. Daubeny, C. W. Bunn, and C. J. Brown, *Proc. Roy. Soc. Lond.,* A226, 531 (1954).
21 W. Ruland, *Acta Cryst.,* 14, 1180 (1961).
22 X. Lu and A. H. Windle, *Polymer,* 36, 451 (1995).

Received July 22, 1997
Revised October 1997